Comparing five and lower-dimensional grain boundary character and energy distributions in copper: experiment and molecular statics simulation

Vadim V. Korolev[a], Jonathan J. Bean[b], Yurii M. Nevolin[c], Yaroslav V. Kucherinenko[d], Keith P. McKenna[e], Pavel V. Protsenko[a,*]

[a]Department of Chemistry, Lomonosov Moscow State University, 119991, Leninskieye Gori, 1-3, Moscow, Russia

[b]Department of Material Science and Metallurgy, The University of Cambridge, Cambridge, CB2 3QZ, UK

[c]Radiochemistry Department, Frumkin Institute of Physical chemistry and Electrochemistry Russian academy of sciences, 117342, Obruchev street, 40, Moscow, Russia

[d]Department of Geology, Lomonosov Moscow State University, 119991, Leninskiye Gory, 1-1, Moscow, Russia

[e]Department of Physics, The University of York, York, YO10 5DD, UK

[*]protsenko@colloid.chem.msu.ru

ABSTRACT

The misorientation of 515 grain boundaries has been determined using electron back scatter diffraction data from an 18 μm thick copper foil with columnar grain structure and a preferential {110} surface orientation. The energy of the grain boundaries was determined from the dihedral angles in the vicinity of grain boundary thermal grooves. The experimental grain boundary energy vs. misorientation angle shows deep minima for the low angle grain boundaries and small minima corresponding to the Σ3 and Σ9 grain boundaries. Only a small fraction of the coincidence site lattice grain boundaries demonstrate an increased occurrence frequency (compared to a random orientation distribution) and low energy. In parallel, the grain boundary energy for a subset of 400 symmetrical tilt grain boundaries was calculated using molecular statics simulations. There is a good agreement between the experiment and molecular statics modeling.

INTRODUCTION

The complex network formed by individual grain boundaries (GBs) has a decisive influence on the physicochemical, mechanical, electromagnetic, and other properties of polycrystalline materials[1]. Understanding the relationship between the crystallographic parameters of GBs and the GB energy has motivated researchers for decades[2–4]. The continuous development of the microelectromechanical systems (MEMS) industry has accelerated the knowledge on how to process devices, which has resulted in different internal interfaces inside the condensed systems[1]. The relationships between degrees of freedom (DOF), GBs structures and GBs energies were investigated previously by many researchers[5–8], but the number of grain boundaries reported in these previous studies are not sufficient to determine the variations of GBs structures and GBs energies in the 5 DOF space. Nevertheless many theoretical models have been proposed to explain this relationship[5,9–12]. Furthermore, in recent years, it has been established that the GBs are also significantly influenced by microscopic degrees of freedom[13] and macroscopically identical GBs can differ significantly by the atomic arrangement in the region between adjacent bulk phases[14].

It is important to verify any theoretical approach or computational model using experimental data on both GB geometry and GB energy for a large set of GBs. The most successful approach to determine experimentally the GB energies considers the equilibrium between the three boundary tensions along the triple line. This equilibrium at triple junctions is described quantitatively by the Herring equation:

- Solid/solid/gas (SSG) capillary equilibrium is established along the line formed by the intersection of the GB plane with the sample surface. The tension of the GB is not balanced by the tensions of free surfaces when the sample surface is flat. Thus, surface deformation occurs and a GB groove is formed. The thermal grooving technique measures the angles in the GB grooves. SSG was previously used for relatively small sets of GBs, most often special GBs with a high degree of symmetry[15–18]. A key requirement for SSG to yield accurate results is that the material should have an isotropic surface energy.
- Solid/solid/solid (SSS) capillary equilibrium. When three GBs join along a common triple line in a polycrystal, the dihedral angles between the corresponding GB planes are determined by capillary equilibrium [19,20]. This equilibrium is established between three capillary vectors. Each capillary vector is a sum of the GB tension vector (lying in the GB plane orthogonal to the triple line) and a torque term vector (equal in absolute value to the derivative of the GB energy with respect to the angle of rotation of the boundary around the triple line and orthogonal to the GB plane and to the triple line). The capillary vector reconstruction method involves solving a system of equations that describe the local equilibrium in triple junctions (Herring equations) using an iterative procedure. Owing to redundancy in the Herring equations, it is necessary to introduce additional restrictions such as constant GB energy within the local domain of the crystallographic GB parameters.

In both SSG and SSS, the objective is to determine the relationship between the GB energy distribution (GBED) and the GB character distribution (GBCD) for all the macroscopic parameters of GBs[4]. SSG and SSS differ only in how the results are generalized from a finite set of GBs to the five macroscopic degrees of freedom of GBs.

In SSG, an extrapolation scheme is used where two important conditions must be met: a reliable set of input data and a suitable functional relationship between the GB energy and crystallographic parameters. The approach proposed by Bulatov[8], where the results of molecular statics simulations for 388 CSL GBs (periodic length for each grain is no more than $15a_0/2$, where a_0 is the lattice spacing) are used as input data[6,7], has become widely used for calculation of GB energy for arbitrary misorientation [21–23]. However, it was demonstrated by comparing the simulated and experimental data that only the Σ3 and Σ9 GBs agree[24].

In the SSS calculation using the Morawiec method, a discretization of the parameter space where the energy is kept constant within each domain is performed. For highly symmetric GBs where the GBED(GBCD) is pronounced, the assumption that the GB energy is constant should be treated with caution and the results of this method strongly depend on the size of the initial sample (filling density) and the size of the domains. Nevertheless, functional dependencies were obtained for a number of materials using this method[25–29]. To cover the parameter space in increments of 10° a set of GBs of approximately 6×10^3 is necessary for cubic symmetry[4]. Recently an update of the Morawiec method was proposed, where the constrain of constant GB energy within each domain was removed[30].

In this paper, we present a comprehensive analysis of a diverse set of GBs in a polycrystalline sample. We have analyzed the dependence between the GBCD and GBED for various subsets of the parameters used to describe the GB structure. It has been possible to interpret the results in the framework of widely used theories, for example the theory of the coincidence site lattice (CSL) and the dependence of the GB energy on the excess free volume. In performing this study, we have found new phenomena such as the presence of an energy minimum for GBs with plane orientation close to (101), a sufficient difference between asymmetrical and symmetrical low index GBs, and the absence of any correlation between GB population and energy. To provide atomistic insights and to ensure consistency in the results, we have also calculated the energies for a similar number of symmetric tilt GBs using the embedded atom method. We believe that our results will be used to construct new extrapolation functions for GBED(GBCD) in future studies.

EXPERIMENT

An electrolytically deposited polycrystalline copper foil of 18 μm in thickness was used to perform the experimental measurements. Disks of 3 mm in diameter were cut from the foil, cleaned with acetone, and annealed in a quartz tube under dry hydrogen flux for 6 h at 1273 K. After the heat treatment, the tube with the sample was quenched in air with a cooling rate between 100 and 200 K/min. The foil samples were characterized with a JSM-840A scanning electron microscope equipped with an electron backscatter diffraction analyzer. Orientation image microscopy© (OIM) maps with 3 μm of spatial resolution were obtained.

The foil surface was investigated using an optical interferometer MII-4 based on the Linnik interference system. Dihedral angles ψ in the vicinity of the GB grooves were measured for 515 GBs using the following technique: The 3D profile of the foil surface, which contains the GB trace (line of intersection between the GB plane and substrate surface), was reconstructed from an interference image of the surface using the interferometer software. Then, five 2D profiles were extracted from the 3D reconstruction for each GB groove perpendicular to the sample surface and the GB trace on the surface. To extract the dihedral angles (ψ), the 2D profiles were fitted using quadratic polynomials through the least squares method (Fig. 1). The dihedral angle ψ between solid surfaces was calculated from an average of five values, measured from the 2D profiles for a given GB. Dihedral angles were measured at a distance of more than 5 μm from the GB triple junctions to avoid the effect of GB groove deformation in the vicinity of the triple point due to the triple point line tension[31].

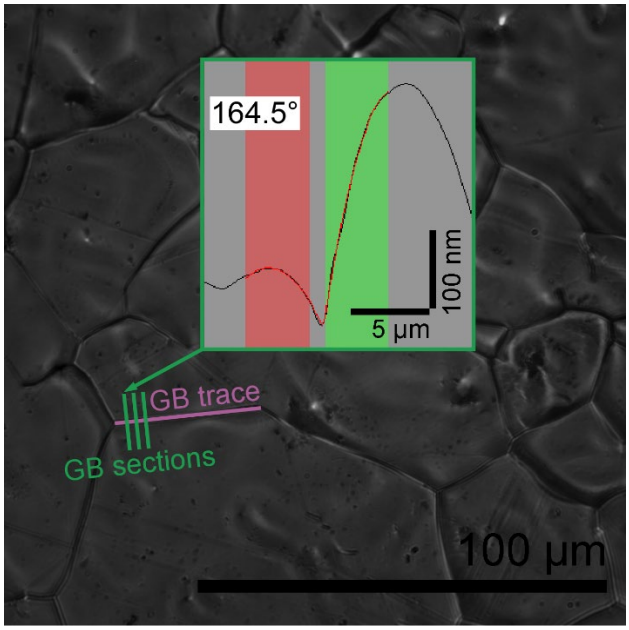

Figure 1. Optical micrograph of foil surface and 2D profile of grain boundary groove fitted with quadratic polynomials to extract dihedral angles ψ (see insert).

To estimate the total error of GB energy measurement, we used the standard technique, which involves a calculation of the average value and the error of the directly measured quantity (dihedral angle in the GB groove), followed by the estimation of the average value and the error of the indirectly measured quantity (GB energy). The absolute error of the dihedral angle measurement $\Delta\psi$ is defined as follows:

$$\Delta\psi = \frac{1}{n}\sum_{i=1}^{n}|\Delta\psi_i| \tag{1}$$

where $\Delta\psi_i$ are the residuals ($\Delta\psi_i = \psi_i - \langle\psi\rangle$) and n is the number of measurements for a given GB (5). Using a first-order Taylor series expansion, the absolute error of the GB energy measurement $\Delta\gamma_{GB}$ can be defined as follows:

$$\Delta\gamma_{gb} = \left|\frac{\partial\gamma_{gb}}{\partial\psi}\Delta\psi\right| \tag{2}$$

By considering the relationship between the GB energy and the solid/liquid interface energy (Eq. 6), and the relative error equation ($\varepsilon_{\gamma_{GB}} = \Delta\gamma_{GB}/\langle\gamma_{GB}\rangle$), the final expression for relative error of the GB energy measurement $\varepsilon_{\gamma_{GB}}$ is equal to

$$\varepsilon_{\gamma_{gb}} = \frac{1}{2}\tan\langle\psi\rangle\,\Delta\psi \quad (3)$$

Thus, the relative error of the GB energy measurement is a nonlinear function of the dihedral angle. For instance, the relative error $\varepsilon_{\gamma_{GB}}$ reaches 0.3 % with a value of ψ = 175° and it equals just 0.1 % for ψ = 165° (the average dihedral angle for all GBs considered).

The error of the instrument is determined by $\frac{\lambda}{2NR}$, where λ is the wavelength of the light source (650 nm), N is the number of treated interference images, and R is a bit depth of the interference images used for profile reconstruction (256). This quantity is negligible compared to the above-considered random error.

Only straight fragments of GB traces were analyzed to minimize the variation of the GB plane orientation within the same boundary. The orientation of GB traces with respect to the sample coordinate system was obtained for 515 GBs. Inspection of the sample surface from both sides reveals that the copper foil has a columnar grain structure with an average grain size of approximately 30 μm (previously reported, Fig. 1a in ref.[32]). It is assumed that the GB planes are perpendicular to the sample surface as their inclination is less than 10°[32].

Both the dihedral angles ψ and the five macroscopic degrees of freedom were obtained for all 515 GBs in the copper foil. Results are compared with those in previous reports on GBED(GBCD) relationships in copper and with molecular statics simulations performed for symmetrical tilt GBs.

MODELING

To investigate the properties of GBs computationally, the energetic stability of 400 symmetric tilt GBs (STGBs) in copper was computed. STGBs are special GBs between two different crystallographic orientations rotated in equal and opposite directions about a common tilt axis. The GB orientations are defined using Miller indices $(hkl)[mno]$, where (hkl) specifies the GB plane and $[mno]$ the tilt axis. Periodic supercells containing two symmetrically equivalent GBs were constructed using the bicrystal approach. The separation between the GBs was set to be greater than 30 Å, which was found to be large enough considering that the mutual elastic interactions are small. Further details of the construction

of STGBs are included in ref.[33]. The structure of the supercells is optimized using the embedded atom method (EAM) description of the interatomic interactions. The total energy of the EAM takes the following form:

$$E_{tot} = \frac{1}{2}\sum_{ij} V(r_{ij}) + \sum_{i} F_i\left(\rho(r_{ij})\right) \quad (4)$$

where $F(\rho)$ is the embedding function, ρ is the density, and V is the pairwise repulsion[34][35]. Here we use the parameterization of Ackland et al., which has been shown to yield very good agreement with experiments for both the structure and associated properties (e.g., mechanical, electronic, or chemical)[33,34,36–39].

To optimize the GBs, the γ surface method was used. This method finds the minimum total energy of the system by performing a series of optimizations from different initial translation states of the two grains relative to each other. The supercells are fully relaxed with respect to the positions of all atoms and the length of the supercell in the GB normal direction. The GB energy γ_{gb} is defined as

$$\gamma_{gb} = \frac{E_{tot} - NE_{coh}}{2A} \quad (5)$$

where E_{tot} is the total energy of the system, N is the number of atoms in the system, and E_{coh} is the cohesive energy of the system. Comparison of GB energy values in copper calculated as described above with values obtained from DFT calculations show divergence up to 35%, relative stability of GBs predicted by EAM and DFT coincides[33].

As there are only three degrees of freedom associated with an STGB, it is possible to perform a mapping from the entire 3D space of possible boundaries to a 2D projection. The 2D projection can then be interpolated to predict the GB energy of an arbitrary STGB. The 2D projection can be intersected to describe all possible GB energy misorientation angles for each different tilt angle. Plots for each specific GB energy/ misorientation are omitted but can be found in the academic literature[5,13]. More details of this approach can be found in the appendices of ref.[33].

RESULTS AND DISCUSSION

The statistical analysis of the grain orientation reveals a strong texture in the $\langle 110 \rangle$ orientation normal to the foil[32]. The same texture was also detected for electrodeposited copper in ref.[21]. To analyze the relationship between GB energy and geometry, the GB energies were extracted from the experimentally measured dihedral angles ψ as follows:

$$\gamma_{gb} = 2\gamma_{sg} \cos\left(\frac{\psi}{2}\right) \tag{6}$$

where γ_{gb} is the GB energy and γ_{sg} is the solid/gas surface energy. Eq. 6 can be used if the solid/gas surface energy γ_{sg} is isotropic. If the surface energy is anisotropic, then the Herring equation[40], included below, should be used instead.

$$\sum_{i=1}^{3} \left(\bar{t}_i \gamma_i + (\bar{t}_i \times \bar{s}) \frac{\partial \gamma_i}{\partial \varphi_i}\right) = 0 \tag{7}$$

where γ_1 and γ_2 are the surface energies of copper crystals forming the planes in the GB, γ_3 is the GB energy, and $\frac{\partial \gamma_i}{\partial \varphi_i}$ are the variations of the surface and GB energies with plane orientation (torque terms). The error introduced from the isotropic approximation can be estimated using anisotropy data of a solid copper surface from the work of D. Chatain et al.[41]. The main result of the Chatain study is presented in the so called γ-plots, where the variance of the crystal surface energy is given. Owing to the presence of the $\{110\}$ texture in our sample[32], we can estimate the maximum values of $\frac{\partial \gamma_{sg}}{\partial \varphi_i}$ from the maximum gradient of the γ-plot close to the $\{110\}$ plane (see Fig. 6 in ref.[41]). This estimation gives $\frac{\partial \gamma_{sg}}{\partial \varphi_i} \leq 19\ \mathrm{mJ/m^2}$, which is approximately 5 % of the average GB energy. To estimate the contribution of torque terms $\frac{\partial \gamma_{sg}}{\partial \varphi_i}$ into γ_{gb} values, Eq. 7 can be simplified to the scalar form for a symmetrical GB groove,

$$\gamma_{gb} = \gamma_1 \cos\left(\frac{\psi}{2}\right) + \gamma_2 \cos\left(\frac{\psi}{2}\right) + \left(\pm \frac{\partial \gamma_1}{\partial x} \pm \frac{\partial \gamma_2}{\partial x}\right) \sin\left(\frac{\psi}{2}\right) \tag{8}$$

If we neglect torque terms $\frac{\partial \gamma_{sg}}{\partial \varphi_i}$ in the calculation of GB energy from the dihedral angle and reduce Eq. 8 to Eq. 6, we obtain a maximum error of 38 mJ/m^2 (approximately 9 % of the

224 average GB energy in our sample). As we have estimated previously [42] the average value of
225 torque term $\frac{\partial \gamma_{gb}}{\partial \varphi_i}$ in copper foil is less than 20% of average GB energy. If we neglect it in the
226 case of columnar structure and isotropic surface energy the error in GB energy determination
227 could be estimated as follows: $\sqrt{1+\left(\frac{\partial \gamma_{gb}}{\partial \varphi_i}/\gamma_{gb}\right)^2}-1$, which is less than 2%. The above
228 concideration allows us to use the relation (Eq. 6) to calculate GB energies. γ_{sg} is estimated
229 for 970°C, and is equal to 1650 mJ/m^2[43], which is in good agreement with data from other
230 sources[44]. The number of GBs studied did not allow us to reveal all the local energy minima
231 in the GBED, but trends for specific subsets of the macroscopic parameters have been found.
232 The range of misorientations is presented in the fundamental zone of Rodrigues-Frank
233 space[45] (Fig. 2). It can be observed in Fig. 2 that the misorientation space is filled with
234 experimental points more or less uniformly, with a slightly higher density of points near Σ3
235 and Σ9 GBs.

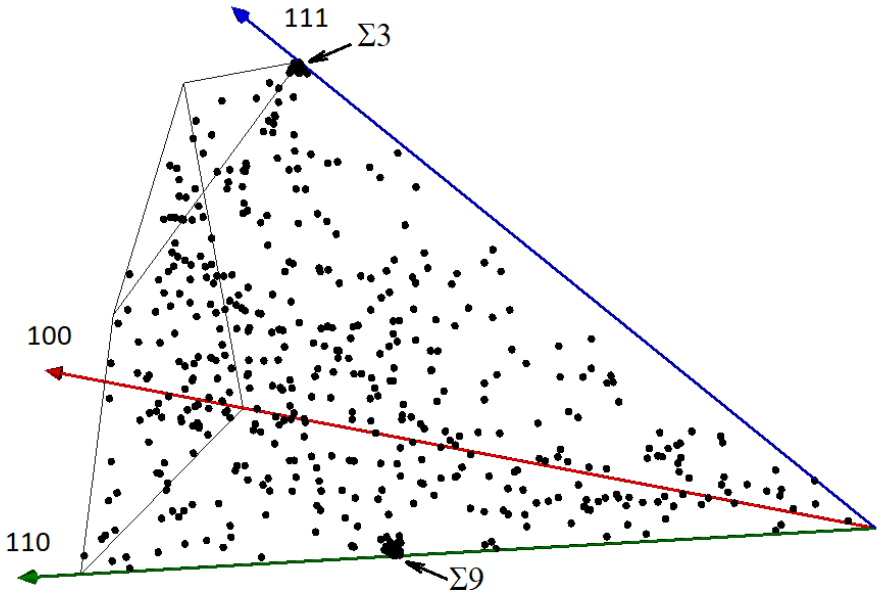

236

237 **Figure 2.** The 515 experimentally determined misorientations represented in the fundamental zone
238 of Rodrigues-Frank space.

239

240 The copper foil under investigation has a pronounced ⟨110⟩ texture, and the GB planes are
241 oriented perpendicular to the foil surface. Only Σ3, Σ9, and Σ27 GBs occurred more
242 frequently in the foil than in the simulated set of GBs, which confirms a special to general

structural transition at the annealing temperature for other CSL misorientations[46]. An analysis of the tilt-to-twist relation did not reveal any specific features compared with a randomly generated GB set, except that the tilt boundaries are enriched due to twinning[32]. GB plane orientation statistics were also analyzed, and it was found that {111} planes were significantly enriched, which can be explained by the foil texture (Fig. 3 in ref.[32]). When compared to a random distribution of grains in an arbitrary cubic crystal, the probabilities of finding GB planes in a ⟨110⟩ textured foil are 1/2 for {111}, 1/3 for {100}, and 1/6 for {110}.

We discuss the effect of GB misorientation (3 DOF) and GB plane orientation (2 DOF) separately. The most straightforward approach is to plot the GB energy vs misorientation angle, ignoring the four other macroscopic DOFs. Rotation by the misorientation angle allows the superposition of elementary cells of adjacent grains; the rotation axis is selected so that the value of the misorientation angle is minimized, thus positioning a given misorientation in the fundamental zone (as shown in Fig. 3). Σ3 and Σ9 GBs are located at 60° and 38.9° correspondingly, but 38-40 and 58-60 column charts contain also general GBs.

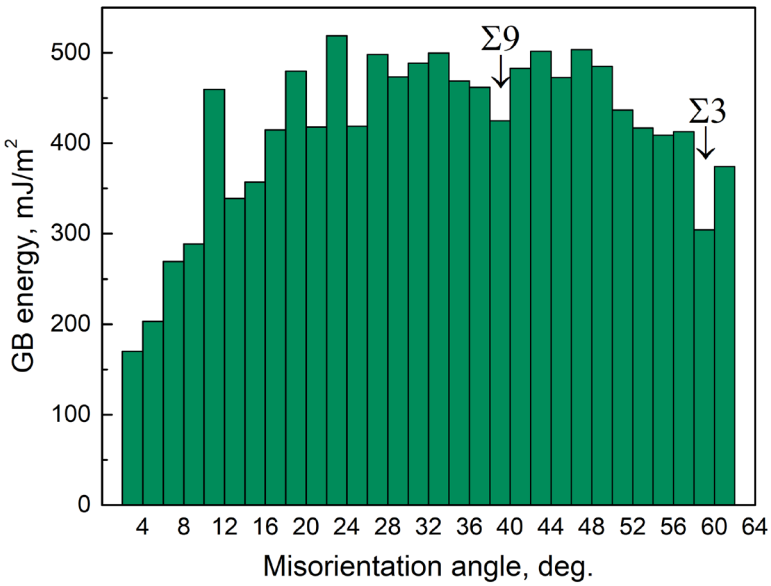

Figure 3. Grain boundary energy vs misorientation angle for the copper foil studied in this work.

The effect of GB plane orientation is determined through the analysis of tilt and twist components. An additional parameter is the angle $\angle(\omega, v)$ between the rotation axis ω and the GB plane normal v[47]. When $\angle(\omega, v)$ is equal to 0°, it is a pure twist boundary, and when it is equal to 90°, it is a pure tilt boundary. Boundaries with $0° < \angle(\omega, v) < 90°$ are known as mixed.

For most misorientations, the average GB energy is constant with a reduction towards angles less than 15°. A quantitative description of the GB energy/misorientation relationship in small angle GBs based on dislocation models was proposed by Read and Shockley[9]. The Read--Shockley model was quantitatively confirmed using highly symmetrical pure tilt or twist GBs and is used to predict energies in pure tilt and twist systems[15]. It is difficult to present mixed GBs as a systematic array of dislocations. An attempt to fit our data with the Read--Shockley equation was made, but in this work, most of the low angle GBs are mixed. We have plotted the GB energy of the low angle GBs in our sample together with data for highly symmetrical GBs from ref.[15] (Fig. 4). All the data are fitted with the Read-Shockley equation.

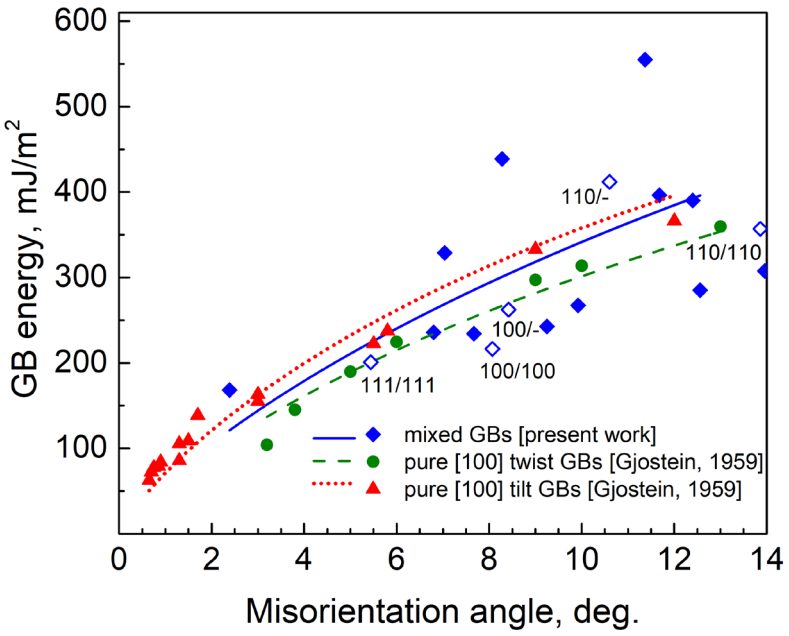

Figure 4. Grain boundary energy of low angle grain boundaries of mixed type (copper foil, 1000°, this study) compared with grain boundary energy of low angle {100} tilt and twist grain boundaries in copper bicrystals at 1065°[15].

The average GB energies for mixed tilt/twist boundaries (our data, blue line) are located between the energies of tilt and twin boundaries determined in ref.[15]. There is a spread of GB energies of approximately hundreds of mJ/mol for mixed GBs, which is much larger than the spread of the energies found in ref.[15] for pure tilt and twist GBs. Our data consists of seventeen GBs with a misorientation angle less than 15°, including three GBs with two low index GB planes, two GBs with one low index plane (empty rhomb), and 12 GBs without low index GB planes (filled rhombs). A low index plane was attributed to a GB if the deviation between the experimentally obtained plane orientation and the low index plane was less than 10°. GBs with two low index planes have relatively low energies, but GBs with only one low index plane have higher energies. The majority of GBs investigated did not contain low index planes, including those with an energy considerably lower than the average value predicted by the Read-Shockley model.

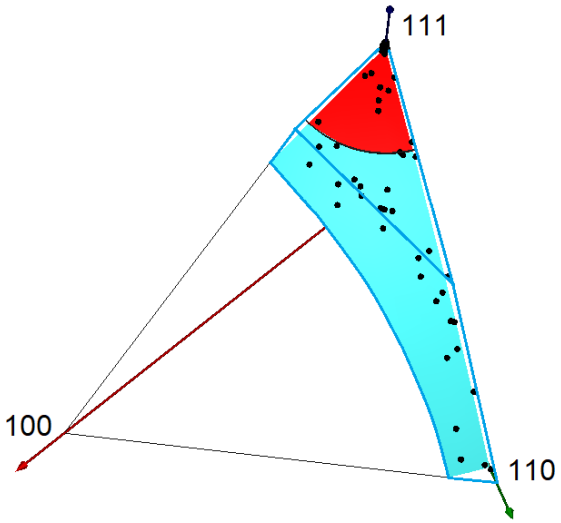

Figure 5. Grain boundaries with misorientation angle 58°–62.8° in Rodrigues-Frank space. The points in the red zone correspond to Σ3 according to the Brandon criterion ($\theta_0 = 15°$).

For high angle GBs, the energy vs misorientation distribution is smooth, except for two mild minima. One minimum is close to 39° and could be linked to the presence of Σ9 GBs and the other minimum is close to 60°, which corresponds to Σ3 GBs. The presence of mild minima close to 39° and 60° is linked to the presence of special (in terms of CSL) GBs. Special GBs in terms of the CSL model (GBs with ≤ Σ35) were selected from the experimental data set.

The Brandon criterion[48] ($\theta_0 = 15°/\sqrt{\Sigma}$) was used to classify GB as "special." A total of 68 % of GBs were identified as Σ3 in the 58°–62.8° misorientation angle range. These GBs are presented as points inside a polygon limited by thick blue lines in the Rodrigues-Frank space (see Fig. 5). In total, 40 % of GBs were identified as Σ9 in the 37°–41° misorientation angle range (see Fig. 3). Σ3 and Σ9 GBs have an average energy value lower than general GBs, and the average Σ3 energy is lower than Σ9.

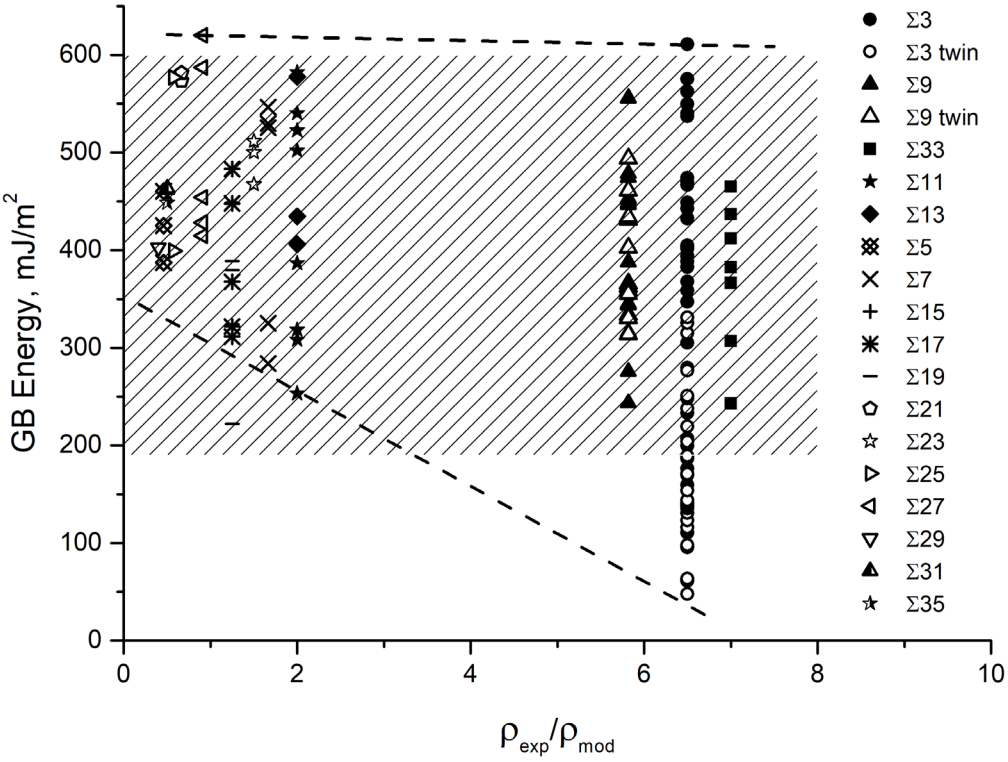

Figure 6. Dependence of grain boundary energy and frequency of occurrence, which is normalized by the frequency generated from random simulation accounting for foil texture. Full range of general grain boundary energy is denoted by hatched area.

The energy of special GBs in terms of the CSL model is plotted against the frequency of their occurrence (ρ_{exp}) in Fig. 6. The frequency of occurrence (ρ_{exp}) was normalized by the frequency of occurrence for the same misorientations in the simulated set of GBs (ρ_{mod}). Grain orientations in ρ_{mod} were generated by considering the $\langle 110 \rangle$ texture of the copper foil[32]. During the microstructure inspection, twins were identified within Σ3 and Σ9 GBs, and they are marked by open cycles and open triangles, respectively. Despite the high occurrence frequency for Σ3, Σ9, and Σ33 GBs, only Σ3 twins have a significantly lower GB

energy. The energy of the other special GBs is not significantly different from the energy of GBs with no Σ value assigned (only ≤ Σ35 were considered). Such GBs should be considered as general in terms of CSL formalism. The result that Σ3 GBs have a lower energy is in good agreement with the hypothesis of "special GBs transition to general ones with increasing annealing temperature[46]." During recrystallization annealing of the copper foil, abnormal grain growth was not observed; thus, the misorientation statistics are close to those of a copper foil with a random distribution of grains taking into account the presence of texture. The sharp increase in Σ3 and Σ9 boundaries could be attributed to the stability of these boundaries during recrystallization, and they decrease in number more slowly than high energy GBs. It should be noticed that number density of Σ9 boundaries (0.062) exceed probability of two Σ3 boundaries meeting ($0.126^2 = 0.016$). Similarly, number density of Σ33 GBs (0.0136) exceed probability of Σ3 and Σ11 meeting (0.126*0.0155 = 0.002)[49].

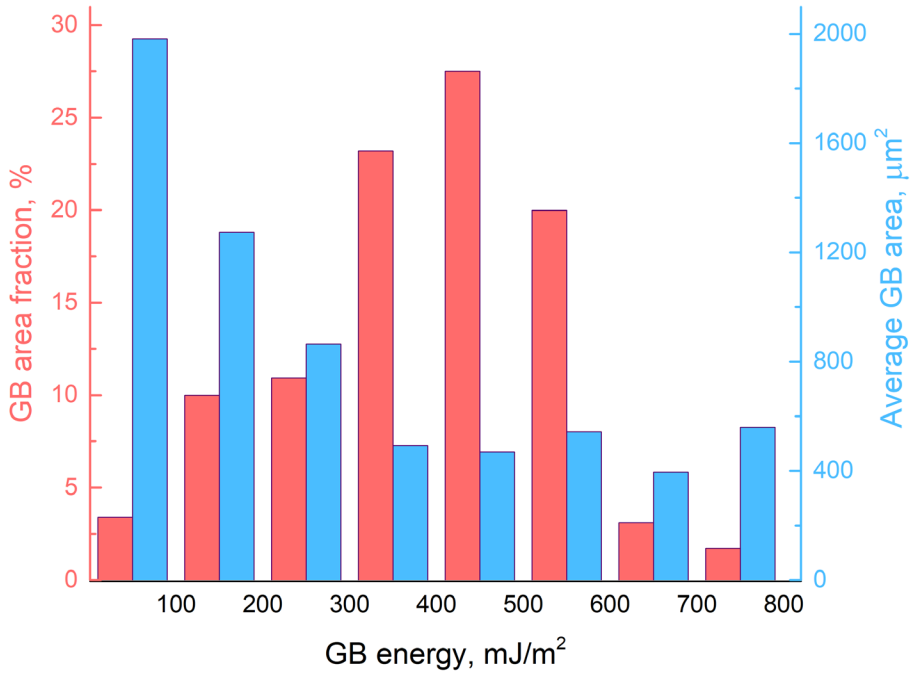

Figure 7. Correlation between the total grain boundary area (red) of each grain boundary fraction and the average area of a single GB (blue) in the corresponding grain boundary energy range.

A strong linear correlation between GB energy and population was reported for polycrystalline nickel[24] and magnesium oxide[6]. A similar correlation was not observed in

the copper foil investigated in this study. It can be observed in Fig. 7 (red) that the maximum GB area fraction corresponds to GBs with an average energy. The distribution in Fig. 7 is asymmetric as GBs with the lowest energy are more frequent than GBs with the highest energy. Such asymmetric behavior can be linked to the grain structure of the copper foil. The area distribution is not in equilibrium and is caused by the initial foil texture. Recrystallization of the copper foil did not lead to a significant structural relaxation towards GBs with a lower surface energy despite 6 h annealing at 1000°C. We believe that the recrystallization is linked to the specific morphology of the foil with {110} texture. For example, in a textured thin film with a columnar structure, not all GB geometries are possible. Those that do occur are relatively more stable than in a 3D polycrystalline sample. During crystallization, the area of the individual boundary grows if the GBs have a low energy and decreases if the GBs have a high energy. This results in the distribution of individual GB areas presented in (Fig. 7).

The misorientation angle alone is not sufficient to describe the energy/misorientation relationship, especially for high angle GBs. A tilt/twist relation defined as the angle between the GB plane normal and the GB misorientation axis was previously suggested as an additional misorientation parameter[16,47]. It was demonstrated in ref.[47] that in FeSi alloys, twist GBs have a higher adsorption capacity for Si atoms. The Krakauer result is in agreement with experimental data presented in ref.[16] where twist GBs have an average energy higher than that of the tilt ones in a NiAl intermetallic polycrystal. In some special cases, twist boundaries were found to have lower energy than tilt GBs with the same misorientation[15].

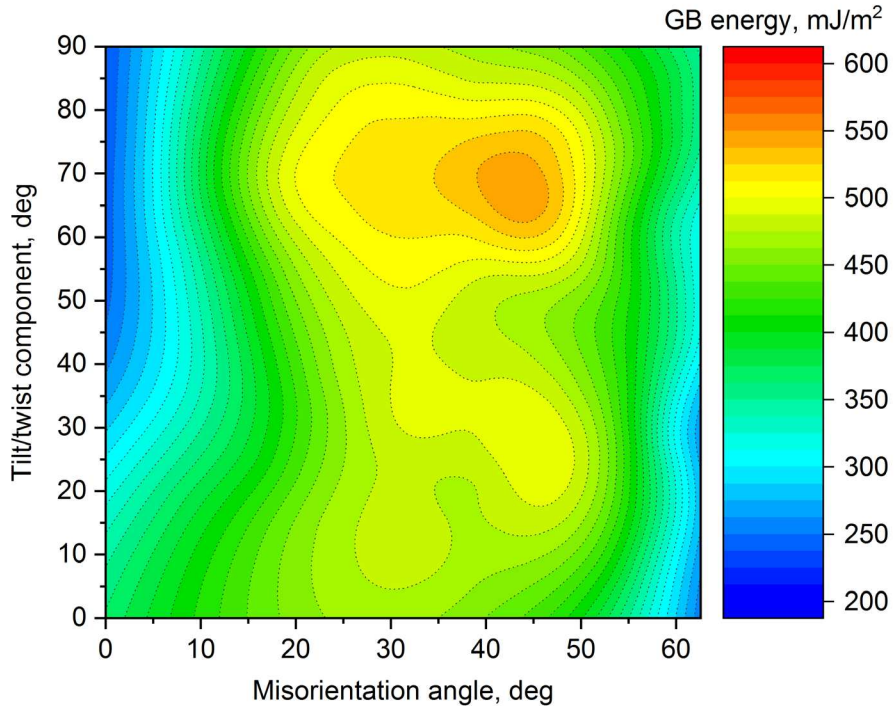

Figure 8. Grain boundary energy as a function of misorientation angle and tilt/twist relation for copper foil.

Variation of the GB energy in the copper foil with a tilt/twist relation and misorientation angle is presented in Fig. 8. The experimental data is fitted with a smooth surface. Low energy GBs are observed at a low misorientation angle and close to 60° misorientation (due to Σ3 {111}/{111} GBs) independent of the tilt/twist relation. At the same time, twist GBs have a slightly lower energy in the entire misorientation range. The region of GBs with the highest energy is situated between 30° and 45° misorientation and at $\angle(\omega, v) = 60° - 80°$. The result of the ranges of angles is in general agreement with experimental data for symmetrical GBs[15] and with the molecular statics simulation of GB energy[6]. The difference between the GB energy of predominantly tilt and predominantly twist GBs is quite weak. This is in agreement with GB statistical data[32].

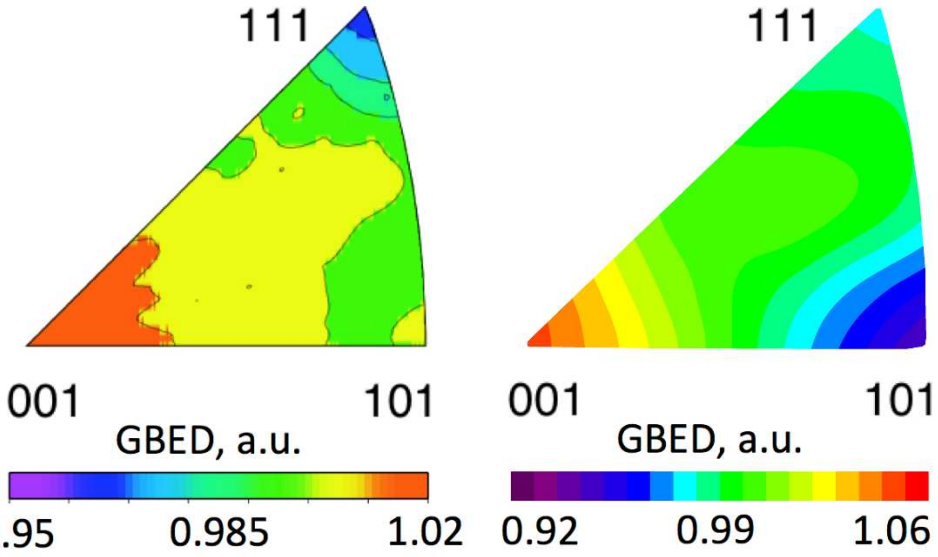

Figure 9. (left) Grain boundary energy distribution as a function of grain boundary plane orientation for nickel[4] (the figure was kindly provided by Prof. G.S. Rohrer, Carnegie Mellon University) and (right) copper (this work).

The influence of GB plane orientation on the GB energy is well established[50,51]. To analyze the GB plane orientation in our copper foil, the GB energy relationship for a large set of mixed GBs in the polycrystal was measured to plot GB energy vs GB plane orientation relative to the crystal lattice of adjacent grains in the form of an azimuthal projection (for example[27]). In the azimuthal projection, each GB is counted twice and misorientation of grains is partially ignored. For example, if one grain is rotated around a GB plane normal, we will obtain different GBs with a similar orientation of the GB plane. In Fig. 9, we compare our data for the copper foil with a similar representation in a nickel polycrystal[4] by means of the Morawiec method[52]. In both cases, copper and nickel, a minimum is observed near the {111} orientation meaning that Σ3 GBs with a low GB energy make a significant contribution into the average GB energy. It is also found that an increase in GB energy is observed for GB plane orientations close to {100} in both copper and nickel. The most important difference between copper and nickel is for GBs close to \{110\}: in the case of nickel, there is no noticeable deviation from the average GB energy value, whereas for copper foil a pronounced minimum was observed.

The variation of the range of average GB energies with plane orientation is insignificant when considering that GB energies vary by more than an order of magnitude depending on

misorientation. In our opinion, considering the GB plane orientations without taking into account grain misorientation will not reveal sharp energy minima in fcc metals. Moreover, the approach described above did not make any distinction between symmetrical and asymmetrical GBs.

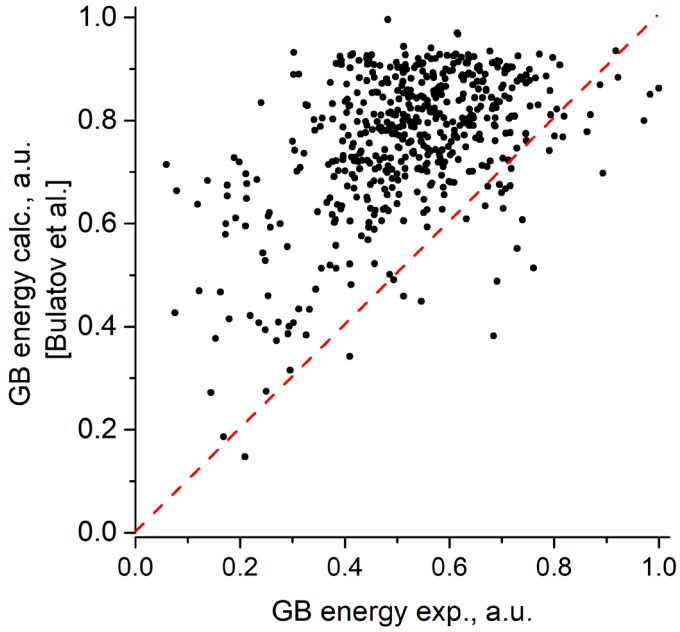

(a)

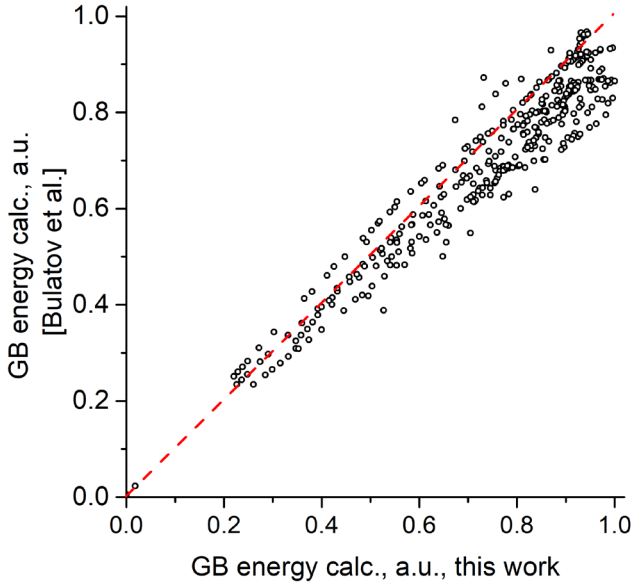

(b)

Figure 10. GB energy values calculated by the function developed in ref.[8] vs those obtained from the experiment with copper foil (a) and calculated by means of molecular statics in this work (b).

It is difficult to cover the 5D space with experimental data, and thus, it is desirable to build a function that determines the GB energy for each misorientation. Recently, a 5DOF function aimed at reconstructing the GBED(GBCD) relationship was suggested[8]. The new 5DOF method uses the energies of 388 GBs in four fcc metals calculated from atomistic simulations using EAM potentials as reference points[6]. GBs considered by Olmsted et al. have periodic length for each grain no more than $15a_0/2$, where a_0 is the lattice spacing. In the present work, we have calculated energies for all GBs from their geometrical parameters using the function developed in ref.[8]. The correlation between the GB energy calculated from dihedral angles ψ in the vicinity of GB grooves and the approximation function of Bulatov et al. (Fig. 10a) is very weak. A similar weak correlation between the experimental and theoretical predictions was observed for nickel[24]. For general GBs in nickel, the correlation between the GB energies simulated in ref.[6] and those determined experimentally in ref.[27] was not observed. Comparison of GB energy values, calculated by molecular statics in this study with values calculated for the same GB parameters by the function presented in [8] is presented in Fig 10b. Good correlation is observed in agreement with the fact that in both cases GBs with short period were modelled.

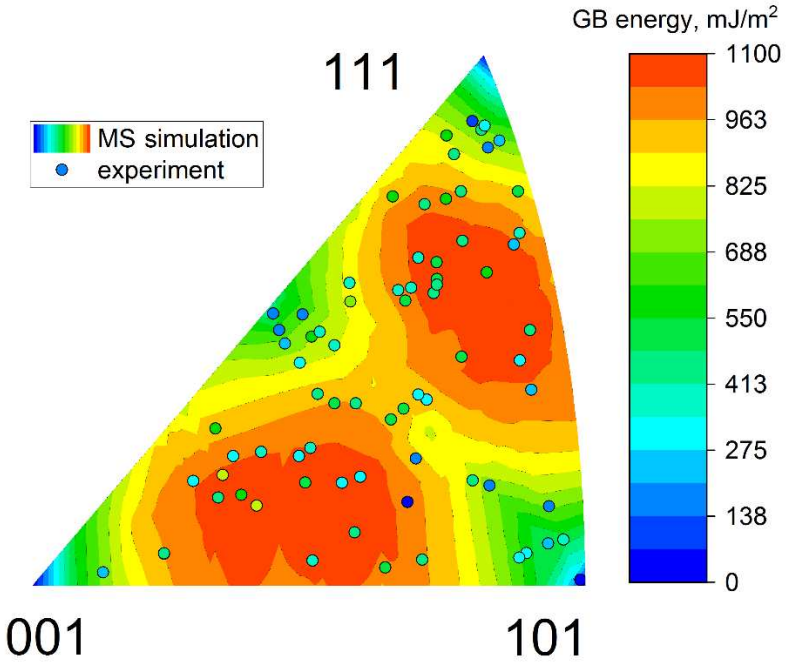

Figure 11. Azimuthal projection of GB plane orientation for 74 symmetrical GBs selected from the experimental data set (cycles) superimposed with GBED obtained by smoothing of molecular statics (MS) calculated values of GB energies for 400 symmetrical tilt GBs in copper.

As presented in Table. 1, GBs that are close to low index planes for one grain only ({111}, {100}, and {110} asymmetrical GBs) have an energy close to the average GB energy. On the contrary, for symmetrical {100}/{100}, {111}/{111}, and {110}/{110} GBs, there is a significant decrease in average GB energy. Even in the {100}/{100} case (there is only one GB of this type, and thus, it is not representative), the GB energy is 1/2 the average GB energy. The energy of GBs combined from different low index planes is higher than the energy of symmetric GBs. Only the {100}/{110} GB demonstrates relatively low energy, but only one GB of this type was found experimentally.

Table 1: Average GB energies and their fraction in the studied GB ensemble for asymmetrical and symmetrical low index GBs in copper foil. Indexes were attributed to the GB plane if its deviation from the given orientation was less than 10°.

GB plane indexes	{100}/—	{111}/—	{110}/—
$\gamma_{gb} / \gamma_{av}$	1.06	1.08	0.97
Fraction of GBs, %	10.2	11.1	10.5
GB plane indexes	{100}/{100}	{111}/{111}	{110}/{110}
$\gamma_{gb} / \gamma_{av}$	0.51	0.62	0.66
Fraction of GBs, %	0.2	1.6	2.0
GB plane indexes	{111}/{100}	{111}/{110}	{100}/{110}
$\gamma_{gb} / \gamma_{av}$	0.93	1.11	0.72
Fraction of GBs, %	2.0	2.0	0.2

The GBED calculated by smoothing of the simulation data for 400 STGBs in copper and the experimental data for a subset of symmetrical GBs from the copper foil are presented in Fig. 11. There is a good agreement between the experimental data and simulation. The simulation demonstrates the presence of four pronounced energy minima close to the {111}, {100}, {110}, and {311} GB planes. These minima correlate with the decrease in free excess

volume, as was previously reported[50]. The experimental data show the same tendency with additional variance and several exceptions. The exceptions are likely related to the inclusion of twist components, which are ignored using this representation. In addition, larger values of GB energy are obtained from the simulation and could relate to the temperature difference (the simulation corresponds to 0 K, whereas the experiment was performed at 1273 K).

For the {111}, {110}, and {311} GB planes, the effect of twist is shown in Fig. 12. It can be observed in Fig. 12 that the twist component has a significant influence on the energy of symmetrical GBs. The most pronounced minima align with the special CSL misorientations Σ3 and Σ9, which is similar for the entire set of studied copper GBs.

CONCLUSIONS

From the work presented in this paper, we can draw several conclusions. First, even for a simple one-component fcc material, a universal relationship between GB energy and GB macroscopic structure is far from being found. Second, in our work, we have identified new subsets of low energy GBs (symmetrical {311}/{311} and {110}/{110}), hence identifying possible avenues to improve the agreement between experiment and theory.

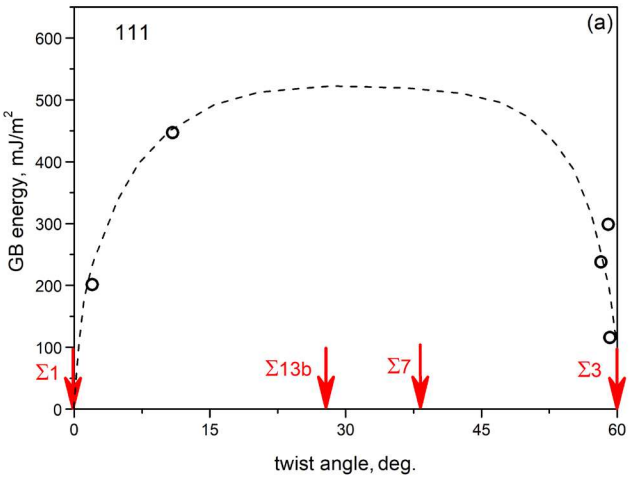

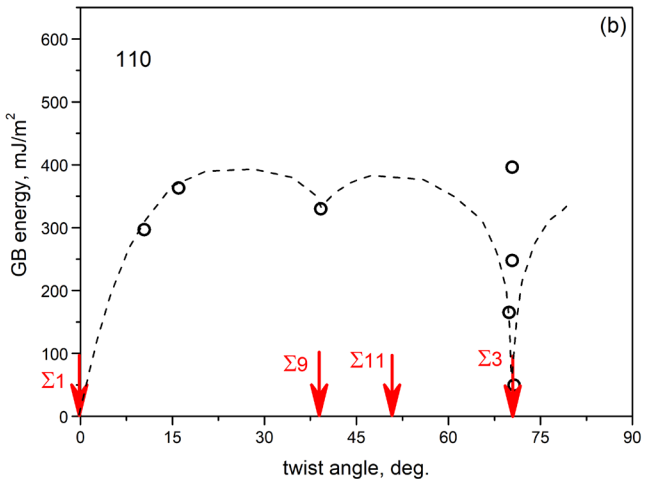

456

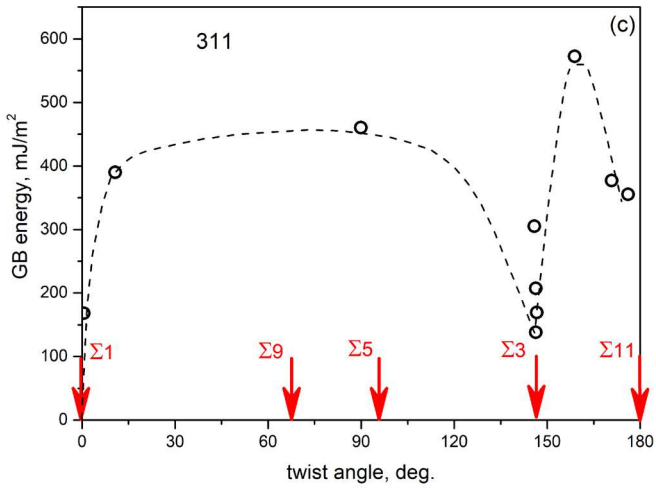

457

458 **Figure 12.** Grain boundary energy for symmetrical GBs vs twist angle for (a) {111}, (b)
459 {110}, and (c) {311} orientations. Deviation from the low index plane is less than 6° for all
460 the presented points.

461

462 To explore the GBED(GBCD) relationship, we have consequentially increased the number of
463 fixed macroscopic degrees of freedom. For example, if we draw energy as a function of
464 misorientation angle (one fixed parameter, Fig. 3) or plane orientation (two fixed parameters,
465 Fig. 9) for our copper foil, it is very difficult to interpret the complexity of the
466 GBED(GBCD) relationship. However, pronounced GB energy minima could be revealed for
467 a subset of symmetrical GBs (four fixed parameters, Fig. 11) and for a subset of symmetrical
468 GBs with a fixed plane orientation as a function of twist angle (five fixed parameters,
469 Fig. 12). This approach minimizes the set of possible assumptions about the functional

dependence between GB energy and its structure. An alternative strategy based on an analytical approximation of the GBED(GBCD) landscape requires a representative set of high-quality data.

The determination of GB energy and excess volume using first-principles calculations within the framework of the density functional theory may provide an adequate base for constructing the energy-structure function. Furthermore, usually GB energies are calculated at 0 K in simulation, and thus, it could be that the calculation of the GB energy at finite temperatures may yield a better relationship between simulation and experiment. At the same time, first-principles calculations are notoriously time consuming and could not be used to reconstruct the full 5-dimensional GBED(GBCD) relationship at the present moment. The data obtained by molecular statics simulation for STGBs are in a good agreement with these experimental findings and understanding the asymmetric effect of GBs could be a compelling follow-on study.

ACKNOWLEDGEMENTS

This work was supported by the Russian Scientific Foundation under grant 19-72-10160. We would also like to acknowledge the financial support from the EPSRC (EP/K003151) and the support from the N8 Consortium (Polaris supercomputer) and the Materials Chemistry Consortium (Archer supercomputer, EPSRC grant EP/L000202). We would also like to acknowledge that part of this work was performed using resources provided by the Cambridge Service for Data Driven Discovery (CSD3) operated by the University of Cambridge Research Computing Service (http://www.csd3.cam.ac.uk/), by Dell EMC and Intel using Tier-2 funding from the EPSRC (capital grant EP/P020259/1), and by DiRAC with funding from the STFC (www.dirac.ac.uk). We give special thanks to Prof A. Lindsay Greer for the useful discussion.

1 T. Watanabe: *J. Mater. Sci.*, 2011, vol. 46, pp. 4095–115.

2 V. Randle: *Acta Mater.*, 1998, vol. 46, pp. 1459–80.

3 V. Randle and G. Owen: *Acta Mater.*, 2006, vol. 54, pp. 1777–83.

4 G.S. Rohrer: *J. Mater. Sci.*, 2011, vol. 46, pp. 5881–95.

5 D. Wolf and S. Phillpot: *Mater. Sci. Eng. A*, 1989, vol. 107, pp. 3–14.

6 D.L. Olmsted, S.M. Foiles, and E.A. Holm: *Acta Mater.*, 2009, vol. 57, pp. 3694–703.

7 E.A. Holm, D.L. Olmsted, and S.M. Foiles: *Scr. Mater.*, 2010, vol. 63, pp. 905–8.

8 V. V. Bulatov, B.W. Reed, and M. Kumar: *Acta Mater.*, 2014, vol. 65, pp. 161–75.

9 W.T. Read and W. Shockley: *Phys. Rev.*, 1950, vol. 78, p. 275.

10 O.B.M. Hardouin Duparc: *J. Mater. Sci.*, 2011, vol. 46, pp. 4116–34.

11 P.R.M. Van Beers, V.G. Kouznetsova, M.G.D. Geers, M.A. Tschopp, and D.L. McDowell: *Acta Mater.*, 2015, vol. 82, pp. 513–29.

12 L. Zhang, Y. Gu, and Y. Xiang: *Acta Mater.*, 2017, vol. 126, pp. 11–24.

13 J. Hickman and Y. Mishin: *Phys. Rev. Mater.*, 2017, vol. 1, p. 010601.

14 T. Frolov, D.L. Olmsted, M. Asta, and Y. Mishin: *Nat. Commun.*, 2013, vol. 4, pp. 1897–9.

15 N.A. Gjostein and F.N. Rhines: *Acta Metall.*, 1959, vol. 7, pp. 319–30.

16 Y. Amouyal, E. Rabkin, and Y. Mishin: *Acta Mater.*, 2005, vol. 53, pp. 3795–805.

17 Y. Amouyal and E. Rabkin: *Acta Mater.*, 2007, vol. 55, pp. 6681–9.

18 S.J. Dillon, M.P. Harmer, and G.S. Rohrer: *J. Am. Ceram. Soc.*, 2010, vol. 93, pp. 1796–802.

19 D.W. Hoffman and J.W. Cahn: *Surf. Sci.*, 1972, vol. 31, pp. 368–88.

20 J.L. Cahn and D.L. Hoffman: *Acta Metall.*, 1974, vol. 22, pp. 1205–14.

519 21 S. Ratanaphan, D. Raabe, R. Sarochawikasit, D.L. Olmsted, G.S. Rohrer, and K.N. Tu:
520 *J. Mater. Sci.*, 2017, vol. 52, pp. 4070–85.

521 22 M.A. Linne, T.R. Bieler, and S. Daly: *Int. J. Plast.*, 2020, vol. 135, p. 102818.

522 23 S.G. Baird, E.R. Homer, D.T. Fullwood, and O.K. Johnson: *Comput. Mater. Sci.*, 2021,
523 vol. 200, p. 110756.

524 24 G.S. Rohrer, E.A. Holm, A.D. Rollett, S.M. Foiles, J. Li, and D.L. Olmsted: *Acta*
525 *Mater.*, 2010, vol. 58, pp. 5063–9.

526 25 D.M. Saylor, A. Morawiec, and G.S. Rohrer: *Acta Mater.*, 2003, vol. 51, pp. 3675–86.

527 26 S.J. Dillon and G.S. Rohrer: *J. Am. Ceram. Soc.*, 2009, vol. 92, pp. 1580–5.

528 27 J. Li, S.J. Dillon, and G.S. Rohrer: *Acta Mater.*, 2009, vol. 57, pp. 4304–11.

529 28 H. Beladi and G.S. Rohrer: *Acta Mater.*, 2013, vol. 61, pp. 1404–12.

530 29 H. Beladi, N.T. Nuhfer, and G.S. Rohrer: *Acta Mater.*, 2014, vol. 70, pp. 281–9.

531 30 Y. Shen, X. Zhong, H. Liu, R.M. Suter, A. Morawiec, and G.S. Rohrer: *Acta Mater.*,
532 2019, vol. 166, pp. 126–34.

533 31 B. Zhao, J.C. Verhasselt, L.S. Shvindlerman, and G. Gottstein: *Acta Mater.*, 2010, vol.
534 58, pp. 5646–53.

535 32 V.V. Korolev, Y.V. Kucherinenko, A.M. Makarevich, B.B. Straumal, and P.V.
536 Protsenko: *Mater. Lett.*, DOI:10.1016/j.matlet.2017.03.076.

537 33 J.J. Bean and K.P. McKenna: *Acta Mater.*, 2016, vol. 110, pp. 246–57.

538 34 M.W. Finnis and J.E. Sinclair: *Philos. Mag. A*, 1984, vol. 50, pp. 45–55.

539 35 M.S. Daw and M.I. Baskes: *Phys. Rev. Lett.*, 1983, vol. 50, p. 1285.

540 36 G.J. Ackland, G.J. Ackland, G. Tichy, V. Vitek, and M.W. Finnis: *Philos. Mag. A*
541 *Phys. Condens. Matter, Struct. Defects Mech. Prop.*, 1987, vol. 56, pp. 735–56.

542 37 F. Cleri and V. Rosato: *Phys. Rev. B*, 1993, vol. 48, p. 22.

543 38 A.P. Sutton and J. Chen: *Philos. Mag. Lett.*, 1990, vol. 61, pp. 139–46.

39 M.S. Daw, S.M. Foiles, and M.I. Baskes: *Mater. Sci. Reports*, 1993, vol. 9, pp. 251–310.

40 H. Gleiter and B. Chalmers: *High-Angle Grain Boundaries*, vol. 16, Pergamon Press Oxford, 1972.

41 D. Chatain, V. Ghetta, and P. Wynblatt: *Interface Sci.*, 2004, vol. 12, pp. 7–18.

42 V.V. Korolev, Y.V. Kucherinenko, and P.V. Protsenko: *Metall. Mater. Trans. A Phys. Metall. Mater. Sci.*, DOI:10.1007/s11661-018-4990-8.

43 N. Eustathopoulos, M.G. Nicholas, and B.B. Drevet: *Wettability at High Temperatures*, vol. 3, 1999.

44 M. Nakamoto, M. Liukkonen, M. Friman, E. Heikinheimo, M. Hämäläinen, and L. Holappa: *Metall. Mater. Trans. B Process Metall. Mater. Process. Sci.*, 2008, vol. 39, pp. 570–80.

45 J. Zhao and B.L. Adams: *Acta Crystallogr. Sect. A*, 1988, vol. 44, pp. 326–36.

46 L.S. Shvindlerman and B.B. Straumal: *Acta Metall.*, 1985, vol. 33, pp. 1735–49.

47 B.W. Krakauer and D.N. Seidman: *Acta Mater.*, 1998, vol. 46, pp. 6145–61.

48 D.G. Brandon: *Acta Metall.*, 1966, vol. 14, pp. 1479–84.

49 K. Miyazawa, Y. Iwasaki, K. Ito, and Y. Ishida: *Acta Crystallogr. Sect. A*, 1996, vol. A52, pp. 787–96.

50 H. Gleiter: *Acta Metall.*, 1970, vol. 18, pp. 23–30.

51 B. Straumal, Y. Kucherinenko, and B. Baretzky: *Rev. Adv. Mater. Sci.*, 2004, vol. 7, pp. 23–31.

52 A. Morawiec: *Acta Mater.*, 2000, vol. 48, pp. 3525–32.

Figure 1. Optical micrograph of foil surface and 2D profile of grain boundary groove fitted with quadratic polynomials to extract dihedral angles ψ (see insert).

Figure 2. The 515 experimentally determined misorientations represented in the fundamental zone of Rodrigues-Frank space.

Figure 3. Grain boundary energy vs misorientation angle for the copper foil studied in this work.

Figure 4. Grain boundary energy of low angle grain boundaries of mixed type (copper foil, 1000°, this study) compared with grain boundary energy of low angle $\{100\}$ tilt and twist grain boundaries in copper bicrystals at 1065°[15].

Figure 5. Grain boundaries with misorientation angle 58°–62.8° in Rodrigues-Frank space. The points in the red zone correspond to Σ3 according to the Brandon criterion ($\theta_0 = 15°$).

Figure 6. Dependence of grain boundary energy and frequency of occurrence, which is normalized by the frequency generated from random simulation accounting for foil texture. Full range of general grain boundary energy is denoted by hatched area.

Figure 7. Correlation between the total grain boundary area (red) of each grain boundary fraction and the average area of a single GB (blue) in the corresponding grain boundary energy range.

Figure 8. Grain boundary energy as a function of misorientation angle and tilt/twist relation for copper foil.

Figure 9. (left) Grain boundary energy distribution as a function of grain boundary plane orientation for nickel[4] (the figure was kindly provided by Prof. G.S. Rohrer, Carnegie Mellon University) and (right) copper (this work).

Figure 10. GB energy values calculated by the function developed in ref.[8] vs those obtained from the experiment with copper foil (a) and calculated by means of molecular statics in this work (b).

Figure 11. Azimuthal projection of GB plane orientation for 74 symmetrical GBs selected from the experimental data set (cycles) superimposed with GBED obtained by smoothing of molecular statics (MS) calculated values of GB energies for 400 symmetrical tilt GBs in copper.

593 **Figure 12.** Grain boundary energy for symmetrical GBs vs twist angle for (a) {111}, (b)
594 {110}, and (c) {311} orientations. Deviation from the low index plane is less than 6° for all
595 the presented points.